

# Thermodynamic and Kinetic Analysis of a Peptide–Class I MHC Interaction Highlights the Noncovalent Nature and Conformational Dynamics of the Class I Heterotrimer<sup>†</sup>

Anne-Kathrin Binz,<sup>‡</sup> Rene C. Rodriguez,<sup>‡</sup> William E. Biddison,<sup>§</sup> and Brian M. Baker<sup>\*,‡</sup>

Department of Chemistry and Biochemistry, University of Notre Dame, 251 Nieuwland Science Hall, Notre Dame, Indiana 46556-5670, and Molecular Immunology Section, Neuroimmunology Branch, National Institute of Neurological Diseases and Stroke, National Institutes of Health, Bethesda, Maryland 20892

Received January 15, 2003; Revised Manuscript Received March 19, 2003

**ABSTRACT:** The class I major histocompatibility (MHC) molecule is a heterotrimer composed of a heavy chain, the small subunit  $\beta_2$ -microglobulin ( $\beta_2$ m), and a peptide. Fluorescence anisotropy has been used to assay the interaction of a labeled peptide with a recombinant, soluble form of the class I MHC HLA-A2. Consistent with earlier work, peptide binding is shown to be a two-step process limited by a conformational rearrangement in the heavy chain/ $\beta_2$ m heterodimer. However, we identify two pathways for peptide dissociation from the heterotrimer: (1) initial peptide dissociation leaving a heavy chain/ $\beta_2$ m heterodimer and (2) initial dissociation of  $\beta_2$ m, followed by peptide dissociation from the heavy chain. Eyring analyses of rate constants measured as a function of temperature permit for the first time a complete thermodynamic characterization of peptide binding. We find that in this case peptide binding is mostly entropically driven, likely reflecting the hydrophobic character of the peptide binding groove and the peptide anchor residues. Thermodynamic and kinetic analyses of peptide–MHC interactions as performed here may be of practical use in the engineering of peptides with desired binding properties and will aid in the interpretation of the effects of MHC and peptide substitutions on peptide binding and T cell reactivity. Finally, our data suggest a role for  $\beta_2$ m in dampening conformational dynamics in the heavy chain. Remaining conformational variability in the heavy chain once  $\beta_2$ m has bound may be a mechanism to promote promiscuity in peptide binding.

The class I major histocompatibility complex (MHC)<sup>1</sup> molecule is a noncovalently linked heterotrimeric complex consisting of a heavy chain, the small subunit  $\beta_2$ -microglobulin ( $\beta_2$ m), and an antigenic peptide typically 8–11 amino acids in length. Class I MHC molecules bind and present antigenic peptides to cell surface T cell receptors; binding of a T cell receptor to a class I peptide–MHC complex is required for initiation and propagation of a cellular immune response. Peptides are bound by the MHC in a groove formed by the heavy chain  $\alpha 1$  and  $\alpha 2$  domains, resulting in a relatively flat surface available for recognition by T cell receptors (1). Antigenic peptides tend to be bound very stably, with affinities typically in the nanomolar range and half-lives of an hour or more (e.g., refs 2 and 3).

There is currently significant interest in quantifying the effects of peptide or MHC substitutions on peptide binding, particularly for those interested in interpreting the effects of peptide or MHC amino acid substitutions on T cell activity or recognition (4–6) or those engaged in peptide vaccine design (7). However, for many MHC alleles, direct measurements of peptide–MHC interactions remain problematic due to slow association and dissociation kinetics and the general instability of the peptide-free heavy chain/ $\beta_2$ m heterodimer (8, 9). Indirect assays of peptide binding, such as competition experiments (2, 10), antibody or receptor binding (6, 11), or thermal denaturation (4, 8, 12, 13), are more common. While such measurements continue to provide useful information such as the rank ordering of affinity or analysis of the effects of mutations on stability, direct measurements of binding allow examination of the underlying interaction kinetics and thermodynamics and allow elucidation of the pathways for assembly and disassembly. Such knowledge is useful in the design and engineering of tight binding peptides as well as ascertaining how MHC mutations or peptide substitutions affect class I MHC assembly, disassembly, and ultimately immunogenicity.

Here, we report the direct measurement of peptide binding and dissociation from the common human class I MHC allele HLA-A2 using fluorescence anisotropy. Experiments were performed with a fluorescently labeled derivative of the high-

<sup>†</sup> Supported by the University of Notre Dame and by Research Grant 1R01GM067079 to B.M.B. from the National Institute of General Medical Sciences, National Institutes of Health. A.-K.B. was supported by a fellowship from the German Academic Exchange Service.

\* Corresponding author. E-mail: bbaker2@nd.edu. Phone: (574) 631-9810. Fax: (574) 631-6652.

<sup>‡</sup> University of Notre Dame.

<sup>§</sup> National Institute of Neurological Diseases and Stroke, National Institutes of Health.

<sup>1</sup> Abbreviations: MHC, major histocompatibility complex; HLA-A2, human leukocyte antigen A\*0201;  $\beta_2$ m,  $\beta_2$ -microglobulin; Tax-3K5Flc, LLKG[K-fluorescein]PVYV; Tax-3K, LLKGYPVYV; Tax, LLFGYPVYV;  $K_D$ , equilibrium dissociation constant;  $k_{on}$ , association rate constant;  $k_{off}$ , dissociation rate constant;  $t_{1/2}$ , dissociation half-life; HC, heavy chain; TS<sup>‡</sup>, transition state.

affinity Tax peptide (sequence LLFGYPVYV) (14). Association measurements were performed using soluble peptide-free HLA-A2 heavy chain/ $\beta_2m$  heterodimer generated from recombinant protein. Our results extend previous studies in the field, which demonstrated that peptide binding to and dissociation from HLA-A2 are both biphasic processes (9). The biphasic association kinetics result from a unimolecular process, attributable to a well-documented conformational transition in the class I MHC heavy chain (9, 15, 16). We show that the biphasic dissociation kinetics, on the other hand, result from two pathways for peptide dissociation: a predominant pathway consisting of peptide dissociation from the fully assembled heterotrimer and a second pathway consisting of initial dissociation of  $\beta_2m$  followed by peptide dissociation from the resulting heavy chain/peptide heterodimer. Eyring analyses of rate constants measured as a function of temperature allow for the first time determination of the enthalpic and entropic components of class I MHC peptide binding. We find that in this case, despite the requirement to fix a flexible peptide, peptide binding is largely entropically driven, likely reflecting the hydrophobic character of the peptide binding groove and the peptide anchor residues.

Finally, our data suggest a role for  $\beta_2m$  in dampening conformational dynamics in the HLA-A2 heavy chain. Remaining conformational variability in the heavy chain/ $\beta_2m$  heterodimer may be a mechanism for promiscuity in peptide binding, as this may permit the heavy chain to make different structural adaptations for different peptides.

## MATERIALS AND METHODS

**Protein Expression and Purification.** Fully assembled HLA-A2 was generated by refolding as previously described (4, 17). Briefly, inclusion bodies for the heavy chain and  $\beta_2m$  were generated separately in *Escherichia coli*. Heavy chain and  $\beta_2m$  inclusion bodies in 8 M urea were diluted to 1 and 2  $\mu$ M, respectively, into refolding buffer (100 mM Tris, 400 mM arginine, 3.7 mM cystamine, 6.3 mM cysteamine, pH 8.3) with 30  $\mu$ M peptide. After incubation for  $\sim$ 24 h at 4 °C, the protein was desalted via dialysis and purified by anion-exchange and size-exclusion chromatography. Excess  $\beta_2m$ , separated at the size-exclusion step, was also collected.

Peptide-free heterodimer was purified by denaturation and fractionation of refolded protein as previously described (8, 9, 13), with simple modifications. Briefly, fully assembled heterotrimer was denatured in 6 M GuHCl, pH 10. Heavy chain,  $\beta_2m$ , and peptide were fractionated using size-exclusion chromatography in 6 M GuHCl, pH 10. High pH was used to aid in denaturation and to ensure stability of the native heavy chain disulfide bonds formed during initial refolding. Fractions containing heavy chain and  $\beta_2m$  were combined and dialyzed against 10 mM HEPES and 150 mM NaCl, pH 7.4, to allow refolding and assembly of peptide-free heavy chain/ $\beta_2m$  heterodimer. After dialysis, samples were filtered and concentrated to 50–100  $\mu$ M, glycerol was added to 20%, and the protein was frozen in aliquots at  $-80$  °C. Purification of peptide-free heterodimer in this fashion is necessary, as attempting to refold HLA-A2/ $\beta_2m$  inclusion bodies in the absence of exogenous peptide results in significant aggregation and precipitation, with no appreciable yield of peptide-free heterodimer (17).

Peptides were synthesized and purified commercially (Sigma-Genosys, Woodlands, TX). For measuring binding and dissociation, a derivative of the Tax peptide (LLFGYPVYV) was used: F3 was substituted with K to increase solubility, and Y5 was substituted with fluorescein-derivatized lysine (peptide referred to as Tax-3K5Flc). Dissociation measurements were performed in the presence of an excess of unlabeled peptide with the sequence LLKGYPVYV (Tax-3K). Extinction coefficients at 280 nM (units of  $M^{-1} cm^{-1}$ ) were 12060 for Tax-3K5Flc, 105600 for HLA-A2/Tax-3K5Flc, 1210 for Tax-3K, 93410 for heavy chain/ $\beta_2m$  heterodimer, and 19180 for  $\beta_2m$ .

**Fluorescence Anisotropy.** Fluorescence anisotropy was measured using a Beacon 2000 fluorescence polarization instrument (PanVera, Madison, WI). The excitation wavelength was 488 nm, and polarization was detected at 535 nm. Polarization was converted to anisotropy as this simplifies data analysis when multiple components are present (18). Data were analyzed using the program Origin (OriginLab, Northampton, MA). Error analysis was performed using standard error propagation techniques (19). Although the Beacon 2000 is not a fast kinetic instrument, it is well suited for equilibrium studies and the relatively slow kinetics observed here. All measurements were performed in 10 mM HEPES and 150 mM NaCl, pH 7.4.

**Peptide Dissociation Kinetics.** Dissociation kinetics were measured with fluorescence anisotropy, using 7.5 nM HLA-A2 loaded with Tax-3K5Flc in the presence of 7.5  $\mu$ M Tax-3K. Dissociation was initiated by manual mixing. Data were fit to single or biphasic decay functions of the form  $y(t) = y_0 + \sum_i (A_i \exp(-k_i t))$ , where  $y_0$  is the baseline offset, the summation is over the number of phases  $i$  (1 or 2),  $k_i$  is the rate constant for phase  $i$ , and  $t$  is the time.

**Equilibrium Binding.** Equilibrium binding of Tax-3K5Flc to peptide-free HLA-A2 heterodimer, also measured using fluorescence anisotropy, was performed at 25 °C with 120 nM peptide-free heterodimer in the presence of 73  $\mu$ M excess  $\beta_2m$  and varying amounts of Tax-3K5Flc. Samples were incubated overnight prior to analysis. Note that because we use anisotropy, data from this experiment differ from that seen in a typical binding isotherm. At high ligand concentration the response is small due to the anisotropy of excess peptide, whereas at low ligand concentration the response is high due to the anisotropy of the heterotrimer.

To fit the data, we took advantage of the fact that anisotropy measures concentration ratios and provides direct information on fraction bound and free (18). At any step in a titration, the observed anisotropy ( $r$ ) is equal to the fraction of ligand bound ( $f_b$ ) multiplied by the anisotropy of the bound state ( $r_b$ ) plus the fraction of ligand free ( $f_f$ ) multiplied by the anisotropy of the free ligand ( $r_f$ ):  $r = f_f r_f + f_b r_b$ . As  $f_f + f_b = 1$ , at any step the fraction bound can be determined from the measured anisotropy as  $f_b = (r - r_f)/(r_b - r_f)$ . The anisotropy of free ligand and saturated protein is readily determined through separate observations. Knowing the fraction bound at any step allows straightforward determination of the concentration of free ligand.

Fraction bound as a function of free peptide was fit to a multiple equal and independent site binding model ( $f_b = nK[\text{Tax-3K5Flc}]/(1 + K[\text{Tax-3K5Flc}])$ ), varying the number of binding sites  $n$  and the equilibrium binding constant  $K$ . Fitting for  $n$  allowed determination of the activity of the

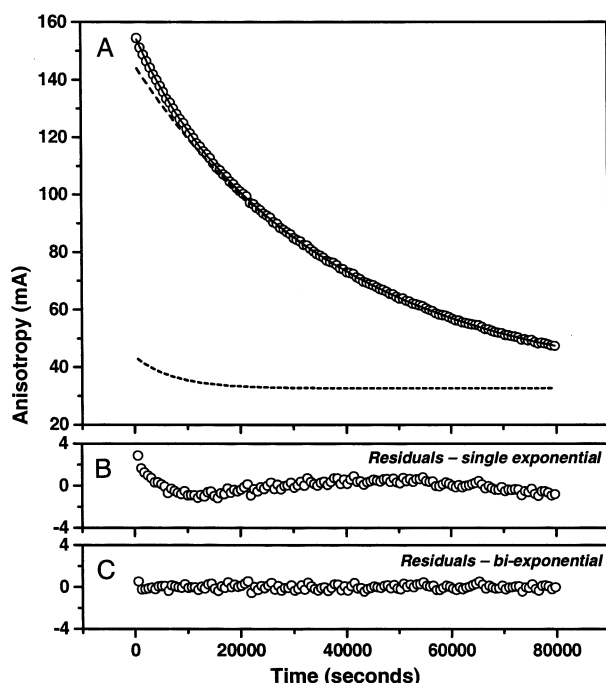


FIGURE 1: Dissociation of Tax-3K5Flc from HLA-A2 is biphasic. (A) Dissociation of Tax-3K5Flc at 25 °C. Data are presented as open circles. The solid line represents a biphasic fit. The dashed lines show peptide dissociation from the heterotrimer (top dashed line) and from the heavy chain/peptide heterodimer (bottom dashed line). (B) Residuals for a monophasic fit to the data in (A), indicating a poor fit. (C) Residuals for the biphasic fit shown in (A), indicating an excellent fit to the data.

heavy chain/ $\beta_2m$  heterodimer. Control experiments varying the concentration of protein with a fixed amount of labeled peptide indicated that fluorescence intensity did not change upon binding.

**Peptide Association Kinetics.** Association kinetics were measured using fluorescence anisotropy under pseudo-first-order conditions, with peptide-free heavy chain/ $\beta_2m$  heterodimer in excess over Tax-3K5Flc. Excess  $\beta_2m$  was present at a concentration of 13  $\mu M$ . Heterodimer concentrations were determined spectrophotometrically and adjusted by the protein activity determined by equilibrium titration; the error in protein activity was propagated to give a value for the error in concentration. Association data were fit to single or biphasic functions of the form  $y(t) = y_0 + \sum_i (A_i(1 - \exp(-k_i t)))$  as described above.

## RESULTS

**Peptide Dissociation Kinetics: Two Pathways for Dissociation.** Figure 1 shows dissociation of Tax-3K5Flc from HLA-A2 at 25 °C. These data did not fit to a single exponential decay (Figure 1B). However, the data were well fit by the sum of two exponentials (Figure 1C). The second phase is characterized by a smaller amplitude and a faster rate. The rate constants for the two phases are  $2.55 \times 10^{-5} s^{-1}$  for the slower phase and  $1.36 \times 10^{-4} s^{-1}$  for the faster phase with the smaller amplitude.

Biphasic dissociation kinetics have been observed previously in measurements of peptide dissociation from both mouse and human class I MHC molecules, including HLA-A2 (9, 15, 20). This has been interpreted as resulting from conformational dynamics in the fully assembled heterotrimer

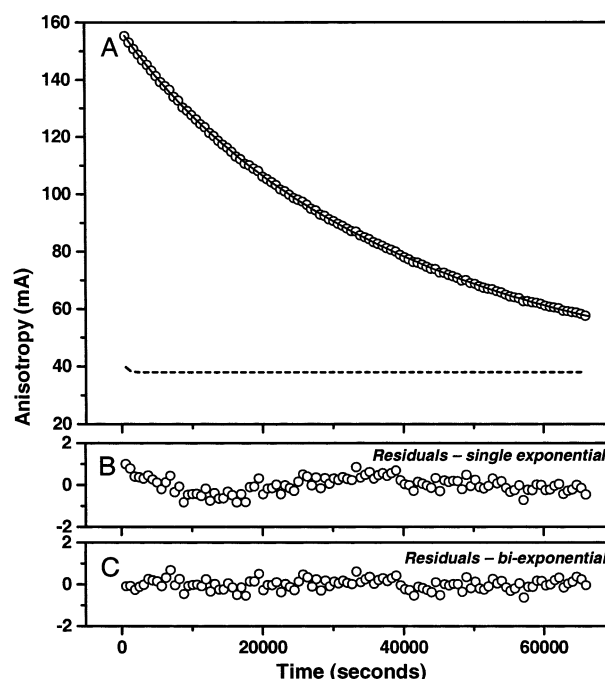


FIGURE 2: Addition of excess  $\beta_2m$  to the dissociation reaction reduces the amplitude of the faster phase. (A) Dissociation of Tax-3K5Flc from HLA-A2 in the presence of excess Tax-3K and excess  $\beta_2m$  at 25 °C. Data are presented as open circles. The solid line represents a biphasic fit. The dashed line indicates peptide dissociation from the heavy chain/peptide heterodimer for comparison with Figure 1A. (B, C) Residuals for mono- and biphasic fits to the data in (A).

(9, 20). We reasoned that an alternative, although not incompatible, interpretation is that the faster phase results from initial dissociation of  $\beta_2m$ , yielding a heavy chain/peptide heterodimer from which peptide more rapidly dissociates. To test this hypothesis, we added a 100-fold excess of  $\beta_2m$  to the dissociation reaction, with the aim of shifting the  $\beta_2m$  dissociation equilibrium toward the fully assembled heterotrimer.

As shown in Figure 2, addition of  $\beta_2m$  to the reaction results in a substantial decrease in the amplitude of the faster phase (a reduction from ~10% to ~5% of the total amplitude; Table 1). However, there is little change in the rate constants characterizing either phase: the rate for the slower phase is  $2.43 \times 10^{-5} s^{-1}$ , and the rate for the faster phase is  $1.25 \times 10^{-4} s^{-1}$  (compare to  $2.55 \times 10^{-5} s^{-1}$  and  $1.36 \times 10^{-4} s^{-1}$  without excess  $\beta_2m$ ; Table 1). This is strong evidence that the biphasic dissociation kinetics results from two routes for peptide dissociation: (1) dissociation of peptide, leaving a heavy chain/ $\beta_2m$  heterodimer, and (2) dissociation of  $\beta_2m$ , resulting in a heavy chain/peptide heterodimer from which peptide then dissociates. As we observe little change in the rate of dissociation through the second route upon addition of  $\beta_2m$ , the decrease in amplitude results from a decrease in the equilibrium population of heavy chain/peptide heterodimer at the start of the experiment, and the rate constant for this phase represents peptide dissociation from the heavy chain/peptide heterodimer.

The amplitudes from these experiments do not allow determination of the relative concentrations of fully assembled heterotrimer and heavy chain/peptide heterodimer at the start of the experiment, as the amplitudes reflect the product of the population of each state and its anisotropy



Table 1: Data for Tax-3K5Flc Dissociation from Fully Assembled HLA-A2<sup>a</sup>

temp (°C)	phase 1: peptide dissociation from heterotrimer			phase 2: peptide dissociation from heavy chain/peptide heterodimer		
	amplitude	$k$ (s <sup>-1</sup> )	$t_{1/2}$ (h)	amplitude	$k$ (s <sup>-1</sup> )	$t_{1/2}$ (h)
4	166.1 ± 3.2	$(1.96 \pm 0.09) \times 10^{-6}$	98.2 ± 4.4			
20	123.5 ± 0.1	$(1.52 \pm 0.04) \times 10^{-5}$	12.7 ± 0.02			
25	113.1 ± 0.5	$(2.55 \pm 0.03) \times 10^{-5}$	7.55 ± 0.10	12.1 ± 0.8	$(1.36 \pm 0.10) \times 10^{-4}$	1.42 ± 0.10
25 <sup>b</sup>	117.2 ± 0.9	$(2.43 \pm 0.07) \times 10^{-5}$	7.92 ± 0.25	6.1 ± 1.7	$(1.25 \pm 0.29) \times 10^{-4}$	1.54 ± 0.36
31	112.3 ± 0.8	$(5.08 \pm 0.10) \times 10^{-5}$	3.79 ± 0.08	20.0 ± 1.2	$(3.7 \pm 0.03) \times 10^{-4}$	0.52 ± 0.04
37	103.6 ± 0.8	$(1.77 \pm 0.04) \times 10^{-4}$	1.09 ± 0.03	18.2 ± 1.2	$(1.4 \pm 0.1) \times 10^{-3}$	0.14 ± 0.01

<sup>a</sup> Data were fit to single exponential (4 and 20 °C) or biexponential (>20 °C) decay functions as described in Materials and Methods. Half-lives are calculated as  $0.693/k$ . <sup>b</sup> Includes a 100-fold molar excess of  $\beta_2m$ .

(18). A heavy chain/peptide heterodimer is expected to have an anisotropy smaller than the heterotrimer but still much larger than the free peptide. Thus the small amplitudes for the second phase in Figures 1 and 2 suggest that the amount of heavy chain/peptide heterodimer is small at 7.5 nM total protein concentration, and we conclude that under the conditions used here peptide dissociation from the fully assembled heterotrimer is the predominant mechanism for peptide dissociation. However, the relative amount of dissociation through either mechanism will depend on protein concentration and the affinity of  $\beta_2m$  for the heavy chain/peptide heterodimer.  $\beta_2m$  affinity for the class I MHC heavy chain/peptide heterodimer has been reported to vary with peptide sequence (21), but this result has recently been questioned (22).

Note that our results are contrary to earlier experiments measuring peptide dissociation from the mouse class I MHC H-2K<sup>d</sup> (20). These authors also observed biphasic dissociation kinetics, but the addition of excess  $\beta_2m$  did not change the relative amplitudes of the phases. The dissimilarity between the two studies may reflect differences between the mouse and human molecules or may reflect differences between experimental approaches.

**Temperature Dependence of Peptide Dissociation.** We next examined the effect of temperature on Tax-3K5Flc dissociation kinetics. In addition to the measurements at 25 °C discussed above, measurements were performed at 4, 20, 31, and 37 °C (Figure 3; data summarized in Table 1). As with the 25 °C data, a biphasic model provided the best fit for the 31 and 37 °C data. In these cases, as at 25 °C, the amplitude of peptide dissociation through the faster route (initial  $\beta_2m$  dissociation, followed by peptide dissociation from the heavy chain/peptide heterodimer) was much smaller than the amplitude for the slower route of dissociation (peptide release from the fully assembled heterotrimer). The observation of monophasic data at 4 and 20 °C may reflect stabilization of the heavy chain/ $\beta_2m$  interface with decreasing temperature.

**Equilibrium Peptide Binding.** Purified peptide-free HLA-A2 heavy chain/ $\beta_2m$  heterodimer was then used with the labeled Tax-3K5Flc peptide in an equilibrium binding assay. In addition to reporting on the overall peptide affinity, this experiment allows determination of the amount of active protein in heavy chain/ $\beta_2m$  preparations. This is necessary for the analysis of peptide binding kinetics under pseudo-first-order conditions when the peptide-free heterodimer is in excess.

Figure 4 shows results from an equilibrium binding experiment for Tax-3K5Flc binding peptide-free HLA-A2

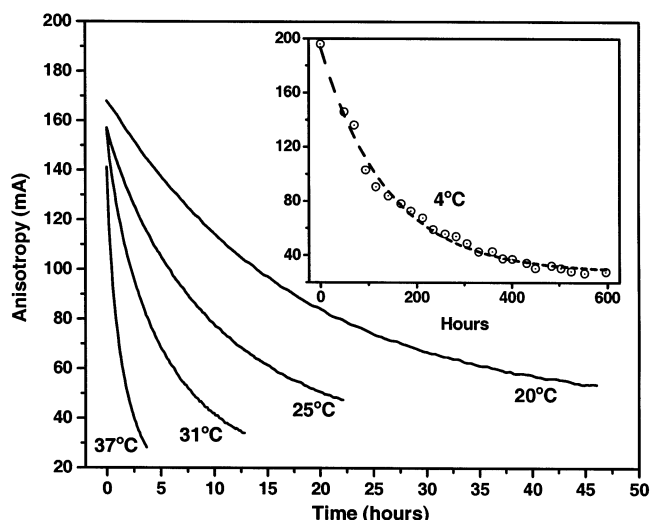


FIGURE 3: Temperature dependence of the kinetics of Tax-3K5Flc dissociation from HLA-A2. Temperatures are indicated. The inset shows data at 4 °C along with a monophasic fit to the data.

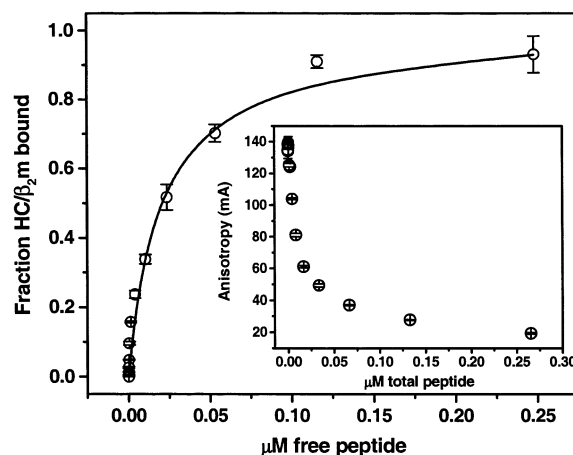


FIGURE 4: Equilibrium binding of Tax-3K5Flc to peptide-free HLA-A2. An increasing amount of Tax-3K5Flc was added to aliquots of 120 nM peptide-free heavy chain/ $\beta_2m$  in the presence of 73  $\mu M$  excess  $\beta_2m$  and the anisotropy measured. Conversion of the raw data (inset) into fraction bound vs concentration of free peptide permitted analysis via a multiple equal and independent site model. The solid line represents a nonlinear fit to this model. Error bars show deviations from three experiments. Values from this fit are  $K_D = 18 \pm 2$  nM and  $n = 0.17 \pm 0.01$ .

heavy chain/ $\beta_2m$  heterodimer. Approximately 600-fold excess  $\beta_2m$  was present to offset the lability of the heavy chain/ $\beta_2m$  heterodimer and minimize the population of heavy chain/peptide heterodimer. The inset to Figure 4 shows the raw data, in which the fully saturated protein has a minimum

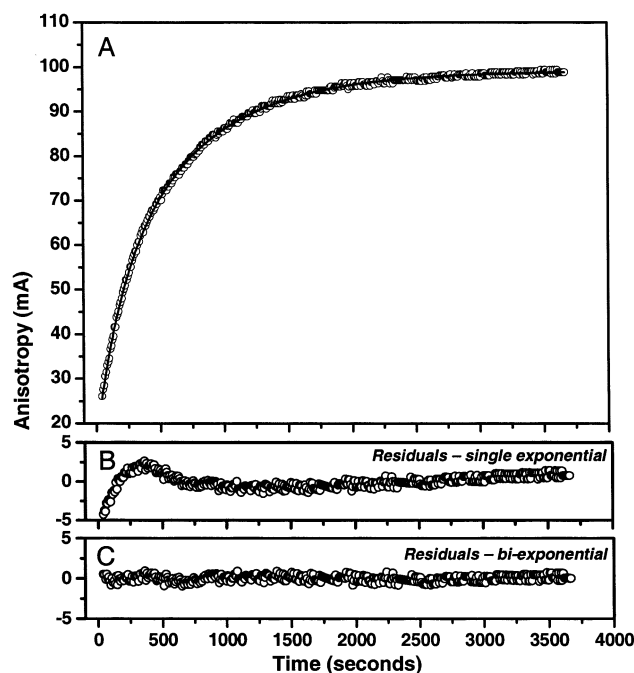


FIGURE 5: Association of Tax-3K5Flc with peptide-free HLA-A2 heavy chain/ $\beta_2m$  is biphasic. (A) Association of 50 nM Tax-3K5Flc with 174 nM HLA-A2 in the presence of 13  $\mu$ M  $\beta_2m$  at 25 °C. Data are presented as open circles. The solid line represents a biphasic fit. (B) Residuals for a monophasic fit to the data in (A), indicating a poor fit. (C) Residuals for the biphasic fit shown in (A), indicating an excellent fit to the data.

anisotropy due to the presence of excess peptide. Transforming these data directly into fraction bound vs concentration of free peptide permits fitting to an independent site binding model varying the number of sites (or protein activity) and affinity.

The resulting  $K_D$  from the average of three experiments is 18 nM, in the range seen for other HLA-A2 tight binding peptides [e.g., 35 nM for the peptide ILKEP[C-dansyl]HGV (9)]. Protein activity was typically near 17%. This activity differs from the value of 80–90% reported by others using a similar procedure to generate peptide-free HLA-A2 heavy chain/ $\beta_2m$  (9). The difference may be attributable to the lability of the heterodimer; different preparations may result in differences in activity due, for example, to differences in protein concentration during dialysis as well as the duration of dialysis. Furthermore, our preparations underwent a freeze–thaw cycle which may negatively impact activity (see Materials and Methods).

**Peptide Association Kinetics.** Association kinetics for Tax-3K5Flc binding to the heavy chain/ $\beta_2m$  heterodimer were measured under pseudo-first-order conditions with the heterodimer in excess, along with additional  $\beta_2m$  to stabilize the heterodimer over the course of the experiment. Measurements were performed at 4, 15, 20, 25, and 31 °C. Data for 25 °C are shown in Figure 5; results for this experiment and experiments at other temperatures are in Table 2. As with the peptide dissociation measurements, association kinetics were biphasic. As has been observed previously (9), the rate constant for one of the phases was insensitive to heavy chain and peptide concentration as well as the ratio of excess  $\beta_2m$  (Table 2), indicating it is an intra- rather than intermolecular event. As has been discussed (9), the most likely origin of this phase is a conformational transition in the HLA-A2

heavy chain from peptide-inaccessible to peptide-accessible conformations. The rate constant we observe for this transition ranges from 0.0006  $s^{-1}$  at 4 °C to 0.008  $s^{-1}$  at 31 °C (Table 2); these values are very similar to those reported by others (i.e., 0.001–0.003  $s^{-1}$  for the temperature range 0–20 °C) (9).

The rate characterizing the second phase was, within error, a linear function of the concentration of peptide-free heavy chain/ $\beta_2m$  heterodimer and independent of peptide concentration, as expected for pseudo-first-order conditions (Table 2). The rate constant describing this phase, reflecting the binding of peptide to the peptide-accessible state of the heterodimer, ranges from  $\sim 5 \times 10^2 M^{-1} s^{-1}$  at 4 °C to  $\sim 1 \times 10^4 M^{-1} s^{-1}$  at 31 °C (Table 2). Thus as previously observed (9), the rate constant for peptide binding shows a greater dependence on temperature than the HLA-A2 conformational transition from peptide-inaccessible to peptide-accessible forms. This may be expected as the association reaction will be dependent upon diffusion, whereas conformational dynamics in the heavy chain will not.

The rate of Tax-3K5Flc binding to the peptide-accessible form of HLA-A2 is similar to rates for peptide binding to class I MHC molecules reported by others (3, 10, 23, 24). However, it is lower than the value of  $\sim 10^5 M^{-1} s^{-1}$  reported by Gakamsky et al., who measured the binding of a dansylated peptide to HLA-A2 (9). Others have measured fast association rates for peptide binding to other class I MHC molecules, i.e., a value of  $\sim 10^6 M^{-1} s^{-1}$  for a peptide binding to an empty form of the mouse class I MHC H-2D<sup>b</sup> (16). In our experiments, the value of  $k_{on}$  is directly proportional to the concentration of active peptide-free HLA-A2 heavy chain/ $\beta_2m$  heterodimer. Thus, errors in protein concentration will directly affect the determined rate constant. However, as the activity of our protein preparation was standardized by equilibrium titration, we conclude that the difference in rate constants reflects intrinsically different association rates for different peptides.

**Eyring Analysis.** Rate constants as a function of temperature for peptide binding and release permit an Eyring analysis for both reactions. Eyring analyses allow, via transition state theory, estimates of activation enthalpy and entropy changes for a reaction (25). Plots of  $\ln k/T$  vs  $1/T$  for peptide binding to the accessible form of the heavy chain/ $\beta_2m$  heterodimer and for peptide dissociation from the fully assembled heterotrimer were both linear, with  $R^2$  values of 0.99 for both plots (figure available as Supporting Information). The transition state thermodynamics for both reactions permits estimates of the overall binding thermodynamics. These values are shown in the form of reaction diagrams in Figure 6. Moving from free peptide to the transition state is enthalpically opposed yet entropically favored, whereas going from the transition state to the bound peptide is favored both enthalpically and entropically. This indicates that the transition state barrier for peptide binding is entirely enthalpic in origin.

The transition state thermodynamics sum to give an overall  $\Delta H^\circ$  of  $-3.0 \pm 2.6$  kcal/mol and a  $\Delta S^\circ$  of  $28.1 \pm 2.1$  cal/(K·mol), indicating that Tax-3K5Flc binding to HLA-A2 is both enthalpically and entropically driven. However, the error in  $\Delta H^\circ$  is large relative to the measurement, and we may consider Tax-3K5Flc binding to be primarily entropically driven. This is consistent with the significant hydrophobic

Table 2: Data for Tax-3K5Flc Association with Peptide-Free HLA-A2 Heavy Chain/ $\beta_2$ m Heterodimer<sup>a</sup>

temp (°C)	[Tax-3K5Flc] (nM)	[heavy chain/ $\beta_2$ m] (nM)	$k_1$ (s <sup>-1</sup> )	$k_{on}$ (M <sup>-1</sup> s <sup>-1</sup> )	$k_2$ (s <sup>-1</sup> )
4	50	217 ± 13	$(1.09 \pm 0.07) \times 10^{-4}$	$(5.03 \pm 0.45) \times 10^2$	$(5.98 \pm 0.39) \times 10^{-4}$
4	50	109 ± 7	$(5.02 \pm 0.17) \times 10^{-5}$	$(4.52 \pm 0.33) \times 10^2$	$(3.87 \pm 0.09) \times 10^{-4}$
15	50	217 ± 13	$(4.60 \pm 0.09) \times 10^{-4}$	$(2.12 \pm 0.14) \times 10^3$	$(2.54 \pm 0.06) \times 10^{-3}$
20	50	217 ± 13	$(6.85 \pm 0.62) \times 10^{-4}$	$(3.14 \pm 0.34) \times 10^3$	$(3.94 \pm 0.02) \times 10^{-3}$
25	50	174 ± 10	$(1.44 \pm 0.02) \times 10^{-3}$	$(8.28 \pm 0.50) \times 10^3$	$(5.25 \pm 0.03) \times 10^{-3}$
25	50	87 ± 5	$(6.84 \pm 0.06) \times 10^{-4}$	$(7.85 \pm 0.47) \times 10^3$	$(4.98 \pm 0.37) \times 10^{-3}$
25	25	87 ± 5	$(7.20 \pm 0.19) \times 10^{-4}$	$(8.81 \pm 0.61) \times 10^3$	$(5.21 \pm 0.10) \times 10^{-3}$
25	13	87 ± 5	$(7.82 \pm 0.30) \times 10^{-4}$	$(8.99 \pm 0.62) \times 10^3$	$(2.76 \pm 0.07) \times 10^{-3}$
31	50	109 ± 7	$(1.14 \pm 0.02) \times 10^{-3}$	$(1.05 \pm 0.06) \times 10^4$	$(8.04 \pm 0.76) \times 10^{-3}$

<sup>a</sup> Data were fit to a biexponential association function as described in Materials and Methods.  $k_{on}$  was determined from  $k_1$  assuming pseudo-first-order conditions.

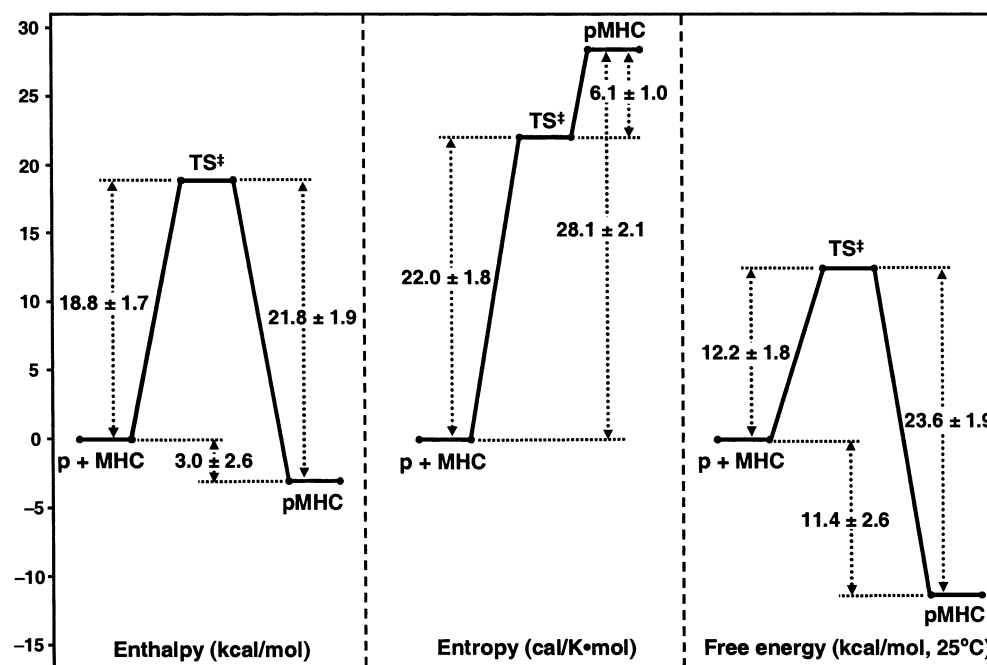


FIGURE 6: Transition state diagram for peptide binding to the accessible form of HLA-A2 and dissociation from the fully assembled heterotrimer (drawn to scale). Comparison of the left and middle panels indicates that the transition state barrier is entirely enthalpic in origin. The differences between the transition state thermodynamics for binding and dissociation permit estimates of the overall binding energetics. Note how the favorable  $\Delta S^\ddagger$  in both directions reduces the free energy barrier for binding *and* increases the free energy barrier for dissociation (right panel).

character of the Tax-3K5Flc peptide and the HLA-A2 peptide binding groove.

Note that this analysis assumes there is no change in heat capacity upon peptide binding. This assumption is likely incorrect and somewhat at odds with the assignment of the positive binding entropy change to the burial of hydrophobic surface (26). However, there is insufficient data to generate a plot of  $\Delta G^\circ$  vs temperature, in which a nonzero  $\Delta C_p$  would be evident as curved line. Thus the values of  $\Delta H^\circ$  and  $\Delta S^\circ$  determined here should be considered best estimates given the available data and the limitations of the system. However, we expect that the effect of a nonzero  $\Delta C_p$  would not qualitatively change our conclusions of a primarily entropically driven reaction. The advantage of the kinetic analysis used here is that the peptide binding reaction can be separated from other reactions that contribute to the total binding  $\Delta G^\circ$ , such as conformational changes in the heavy chain.

## DISCUSSION

**Peptide Binding Thermodynamics.** The Eyring analysis used here represents, to our knowledge, the first time the

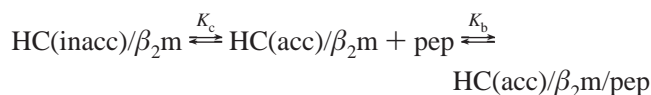
thermodynamics underlying peptide binding have been determined for a class I MHC–peptide interaction. Although we can expect the thermodynamics to differ for different peptide–MHC combinations, there are some generalizations that can be made, such as the role of the hydrophobic effect in peptide binding. The use of a gain in solvent entropy from the burial of hydrophobic groups to offset the reduction in peptide conformational entropy that occurs upon binding has been observed in other peptide–recognition systems (27). We might expect similar results for other peptides that bind HLA-A2, given the requirement for bulky, hydrophobic amino acids at the primary anchor positions (28).

The transition state thermodynamics are consistent with recent conceptual descriptions of protein–ligand transition states, i.e., a loosely packed, partially dehydrated interface (29). The enthalpic barrier to binding may result from the stripping of water from partial and full charges on the peptide and MHC, as well as the reduction in the favorable hydrogen bond enthalpy associated with hydrophobically “oriented” water (26). As the transition state settles into the bound state,

some favorable enthalpy is regained as peptide–MHC hydrogen bonds and salt bridges are formed, although a number of such interactions may already be formed at the transition state (29). If we assume the interface at the transition state is partially dehydrated, then entropically, formation of the transition state from the unbound components again reflects the hydrophobic effect as waters are released. Forming the bound state from the transition state requires release of further water, giving rise to additional entropy.

Entropy also plays a significant role in influencing the kinetics of the peptide–MHC reaction. Note from Figure 6 how the entropy component of the transition state thermodynamics simultaneously reduces the activation barrier for binding and increases the barrier for dissociation (Figure 6, compare left and right panels). This demonstrates an intriguing entropic component of the mechanism by which tight peptide binding and slow dissociation are achieved. Studies with additional peptides and MHC alleles are necessary to ascertain the generality of these results.

**Conformational Dynamics in HLA-A2 Assembly.** An important aspect of the class I MHC molecule is that peptide binding proceeds via a conformational transition in the heavy chain from peptide-inaccessible to peptide-accessible forms. This has been well documented (9, 15, 16), but our observations permit a more complete analysis of the role of conformational dynamics in the assembly of the molecule. Considering only the interaction of the peptide with the heavy chain/ $\beta_2m$  heterodimer, peptide binding can be described by the mechanism:



where  $K_c$  is the equilibrium constant describing the conversion of the heavy chain (HC) from the peptide-inaccessible (inacc) to peptide-accessible (acc) forms and  $K_b$  is the equilibrium constant describing peptide binding to the accessible form. From this model, the overall (i.e., observed) equilibrium constant ( $K_{\text{obs}}$ ) for peptide binding to the heterodimer is

$$K_{\text{obs}} = \frac{K_c}{1 + K_c} K_b$$

For Tax-3K5Flc binding HLA-A2, we have measured a value of  $5.6 \times 10^7 \text{ M}^{-1}$  for  $K_{\text{obs}}$  (equal to  $1/18 \text{ nM}$  at  $25^\circ\text{C}$ ; see Figure 4), and  $K_b$  is equal to  $3.3 \times 10^8 \text{ M}^{-1}$  (equal to the average value of  $k_{\text{on}}$  over  $k_{\text{off}}$  at  $25^\circ\text{C}$ ; Tables 1 and 2). This gives a value of 0.2 for  $K_c$ , implying that, at least at  $25^\circ\text{C}$ , only  $\sim 17\%$  of heavy chain/ $\beta_2m$  heterodimers are in the peptide-accessible form. As this is a unimolecular reaction and the rate constant for conversion from inaccessible to accessible forms varies only slightly with temperature, we might expect a similar ratio at physiological temperatures.

$\beta_2m$  dissociation from the fully assembled complex yields a heavy chain/peptide heterodimer. Although peptide dissociation from this heterodimer is faster than peptide dissociation from the fully assembled heterotrimer (Table 1), it is still slow, with a value of  $\sim 1.3 \times 10^{-4} \text{ s}^{-1}$  at  $25^\circ\text{C}$  (half-life of  $\sim 1.5 \text{ h}$ ). This indicates that once bound, the

peptide is almost as tightly held by the free heavy chain as it is by the heavy chain/ $\beta_2m$  heterodimer. Nevertheless, peptide binding to free HLA-A2 heavy chains occurs very slowly (9). One possible reason is that the free heavy chain populates a variety of conformations, of which only a small subset is peptide-accessible. Binding of  $\beta_2m$  to the heavy chain must shift the heavy chain conformational equilibrium further toward the peptide-accessible conformation(s), although as discussed above, the equilibrium still lies toward the inaccessible state(s) by  $\sim 83\%$ .

Unlike peptide,  $\beta_2m$  on the other hand binds rapidly to free HLA-A2 heavy chains (9). This suggests the heavy chain conformational variability lies mostly in the peptide binding domain. However, there must be further communication between  $\beta_2m$  and peptide binding, or the peptide dissociation rates from the heavy chain/peptide heterodimer and the fully assembled heterotrimer would be the same, rather than the approximate order of magnitude difference we observe here (Table 1).

The ability of  $\beta_2m$  to shift the heavy chain conformational equilibrium toward the peptide-accessible state(s) suggests a role for  $\beta_2m$  in acting as a conformational “damper” for the heavy chain that acts to promote peptide binding. Remaining conformational variability in the heavy chain after  $\beta_2m$  binding may be a mechanism for promiscuous peptide binding by class I MHC molecules, as this will allow the peptide binding domain to adapt to different peptides. Structures of the same class I MHC molecule with different peptides often exhibit small conformational differences in the peptide binding domain (e.g., refs 30 and 31). Such differences are often referred to as conformational changes “induced” by peptide binding but can equally be described as peptide binding to the heavy chain conformation that provides the best energetic “fit” to the peptide. Following this reasoning, we might expect different values of the population of heavy chain in the peptide-accessible form ( $K_c$  in the above model) for different peptides. Remaining conformational variability in the heavy chain after  $\beta_2m$  has bound provides an explanation for the decreased thermal stability and molten globule characteristics of peptide-free class I MHC molecules (8, 13).

## ACKNOWLEDGMENT

We thank Drs. Patricia L. Clark and Kenneth P. Murphy for helpful advice and comments on the manuscript.

## SUPPORTING INFORMATION AVAILABLE

Eyring plots of Tax-3K5Flc binding to the peptide-accessible form of HLA-A2 and dissociation from the fully assembled complex. This material is available free of charge via the Internet at <http://pubs.acs.org>.

## REFERENCES

1. Bjorkman, P. J., Saper, M. A., Samraoui, B., Bennett, W. S., Strominger, J. L., and Wiley, D. C. (1987) *Nature* 329, 506–512.
2. Fahnestock, M. L., Johnson, J. L., Feldman, R. M., Tsomides, T. J., Mayer, J., Narhi, L. O., and Bjorkman, P. J. (1994) *Biochemistry* 33, 8149–8158.
3. Sette, A., Sidney, J., del Guercio, M. F., Southwood, S., Ruppert, J., Dahlberg, C., Grey, H. M., and Kubo, R. T. (1994) *Mol. Immunol.* 31, 813–822.



4. Baker, B. M., Turner, R. V., Gagnon, S. J., Wiley, D. C., and Biddison, W. E. (2001) *J. Exp. Med.* 193, 551–562.
5. Wang, Z., Turner, R., Baker, B. M., and Biddison, W. E. (2002) *J. Immunol.* 169, 3146–3154.
6. Holler, P. D., Lim, A. R., Cho, B. K., Rund, L. A., and Kranz, D. M. (2001) *J. Exp. Med.* 194, 1043–1052.
7. Sliz, P., Michielin, O., Cerottini, J.-C., Luescher, I., Romero, P., Karplus, M., and Wiley, D. C. (2001) *J. Immunol.* 167, 3276–3284.
8. Bouvier, M., and Wiley, D. C. (1998) *Nat. Struct. Biol.* 5, 377–384.
9. Gakamsky, D. M., Davis, D. M., Strominger, J. L., and Pecht, I. (2000) *Biochemistry* 39, 11163–11169.
10. Matsumura, M., Saito, Y., Jackson, M. R., Song, E. S., and Peterson, P. A. (1992) *J. Biol. Chem.* 267, 23589–23595.
11. Rudolph, M. G., Speir, J. A., Brunmark, A., Mattsson, N., Jackson, M. R., Peterson, P. A., Teyton, L., and Wilson, I. A. (2001) *Immunity* 14, 231–242.
12. Khan, A. R., Baker, B. M., Ghosh, P., Biddison, W. E., and Wiley, D. C. (2000) *J. Immunol.* 164, 6398–6405.
13. Fahnestock, M. L., Tamir, I., Narhi, L., and Bjorkman, P. J. (1992) *Science* 258, 1658–1662.
14. Koenig, S., Woods, R., Brewah, Y., Newell, A., Jones, G., Boone, E., Adelsberger, J., Baseler, M., Robinson, S., and Jacobson, S. (1993) *J. Immunol.* 151, 3874–3883.
15. Gakamsky, D. M., Boyd, L. F., Margulies, D. H., Davis, D. M., Strominger, J. L., and Pecht, I. (1999) *Biochemistry* 38, 12165–12173.
16. Springer, S., Doring, K., Skipper, J. C., Townsend, A. R., and Cerundolo, V. (1998) *Biochemistry* 37, 3001–3012.
17. Garboczi, D. N., Hung, D. T., and Wiley, D. C. (1992) *Proc. Natl. Acad. Sci. U.S.A.* 89, 3429–3433.
18. Jameson, D. M., and Sawyer, W. H. (1995) *Methods Enzymol.* 246, 283–300.
19. Bevington, P. R., and Robinson, D. K. (1992) *Data reduction and error analysis for the physical sciences*, 2nd ed., McGraw-Hill, New York.
20. Gakamsky, D. M., Bjorkman, P. J., and Pecht, I. (1996) *Biochemistry* 35, 14841–14848.
21. Parker, K. C., DiBrino, M., Hull, L., and Coligan, J. E. (1992) *J. Immunol.* 149, 1896–1904.
22. Horig, H., Papadopoulos, N. J., Vegh, Z., Palmieri, E., Angeletti, R. H., and Nathenson, S. G. (1997) *Proc. Natl. Acad. Sci. U.S.A.* 94, 13826–13831.
23. Ojcius, D. M., Godeau, F., Abastado, J. P., Casanova, J. L., and Kourilsky, P. (1993) *Eur. J. Immunol.* 23, 1118–1124.
24. Chen, W., Khilko, S., Fecondo, J., Margulies, D., and McCluskey, J. (1994) *J. Exp. Med.* 180, 1471–1483.
25. Eyring, H. (1935) *Chem. Rev.* 17, 65–77.
26. Baker, B. M., and Murphy, K. P. (1998) *Methods Enzymol.* 295, 294–315.
27. Murphy, K. P., Xie, D., Garcia, K. C., Amzel, L. M., and Freire, E. (1993) *Proteins* 15, 113–120.
28. Falk, K., Rotzschke, O., Stevanovic, S., Jung, G., and Rammensee, H. G. (1991) *Nature* 351, 290–296.
29. Gabdoulline, R. R., and Wade, R. C. (2002) *Curr. Opin. Struct. Biol.* 12, 204–213.
30. Madden, D. R., Garboczi, D. N., and Wiley, D. C. (1993) *Cell* 75, 693–708.
31. Fremont, D. H., Matsumura, M., Stura, E. A., Peterson, P. A., and Wilson, I. A. (1992) *Science* 257, 919–927.

BI034077M